Biochemistry Letters, 13(4) 2018, pages 40-53

Scientific Research & Studies Center-Faculty of Science- Zagazig University- Egypt

Biochemistry Letters

Journal home page:

In vitro antibacterial and bio-histological effects of *cerastes cerastes* venom on albino mice

Amany M. Shabaan*[1], Abir A. El Feky[2], Abdel Karim M. Abdel Latif[3], Huda K. Moghib[3]

***1*-. Chemistry Department, Bio-Chemistry Division, Faculty of Science, El Fayoum University, El-Fayoum, Egypt.**

***2*- Applied venom Research Sector- Egyptian Organization for biological products and vaccines, Egypt.**

***3*- Zoology Department, Faculty of Science, El Fayoum University, El- Fayoum, Egypt.**

ARTICLE INFO

Article history:
Received :
Accepted :
Available online :

Keywords: *Cerastes cerastes, LD_{50}, serum biochemical, histopathology, toxicity, antibacterial effect.*

ABSTRACT

Background: Snake venoms contain mixtures of proteins that have different pathological and pharmaceutical effects. In the present study, we evaluated, in vitro the anti-bacterial activity of *Cerastes cerastes* (*C. cerastes*) crude venom. Results revealed it has broad antibacterial activity against *S. typhimurium* and *S. aureus*, and resistant to *E. coli*. In vivo, we analyzed the biochemical and histological effects of the sublethal dose of the venom. 45 Swiss albino mice were divided into 3 groups (15 mice/ group): control group; 1/10 LD50 group and 1/2 LD_{50} group. Mice were dissected 48 hours after the injection and blood were collected. CBC, ALT, AST, urea, creatinine, total CPK, and LDH were measured. Histopathological changes induced by the venom in skin, liver, heart and kidney tissues were examined. A significant increase in RBCs in 1/10 LD50 group, while a significant decrease of which in 1/2 LD_{50} group was observed. Thrombocytopenia, Leukocytosis and highly significant increase in monocytes were observed in both treated groups during the study. A significant increase was observed for lymphocytes and neutrophils in 1/2 LD_{50} group. Serum levels of AST, ALT, urea, creatinine, total CPK and LDH were highly increased in both envenomed groups. The histopathological changes in liver, heart, skin and kidney tissues indicated that venom has hemotoxic effect in mice.

© 2018 Publisher All rights reserved.

INTRODUCTION

Snakebite comprises an ignored broad medical problem worldwide; its risk is higher in the tropics and West Africa, most of whom are rural (1). The horned viper *Cerastes cerastes* is one of the most poisonous snakes in Egyptian deserts. It belongs to the family Viperidae and known as pragmatic predators with varied diets (2).

Viper venoms contain a mixture of biologically active proteins responsible for various pathological effects of hemorrhage, thrombosis and tissue damage to vital organs (3). Its venom also causes significant physio-

pathological changes in liver, heart, and skin (4). In spite of its pathological effects, several proteins of which have practical applications as pharmaceutical agents (5).

Bacterial infection involving the multidrug resistant strains becomes one of the 10 leading causes of death worldwide. The health care system worldwide has suffered an extraordinary burden in terms of searching for new and stronger antimicrobial compounds (6). Given its vast ability as the source of therapeutics, it was found that viper venom has antimicrobial activity against gram-positive and gram-negative bacteria (7). The venom antimicrobial activity was due to enzymes such as L-amino acid oxidase (8).

The objectives of the present study are to investigate the antibacterial activity of *Cerastes cerastes* crude venom against Gram-negative bacteria (*Escherichia coli* and *Salmonella typhimurium*), as well as Gram-positive bacteria (*Staphylococcus aureus)*. Also, unveiled on the histopathological and biochemical alterations induced in envenomed mice with sub-lethal doses 1/10 LD_{50} and 1/2 LD_{50} of *Cerastes cerastes* venom.

2. *Materials and Methods*.

Venom preparation:

The lyophilized crude venom of adult horned viper (*Cerastes cerastes*) was obtained from ANDICOE, VACSERA and stored in the brown vial at refrigerator (4°C) till used.

Determination of LD_{50} dose:

LD_{50} of crude venom was determined according to (9). Concisely, LD_{50} of the venom was determined by injection of different concentrations of venom in 0.5 ml of normal saline intravenously in albino Swiss mice. Five mice were used per group for each dose. Dose increasing factor was 1.2 for each group until 50% mortality was observed within 24 h. The LD_{50} of venom was obtained to be 0.535 mg/kg body weight.

Bacterial strains

The Gram-positive bacteria including *Staphylococcus aureus* (ATCC: 29213) and Gram-negative bacteria including *Salmonella typhimurium* (ATCC: 35664) and *Escherichia coli* (ATCC: 25922) were kindly obtained from American Type Culture Collection number.

Inoculums Preparation:

A loopful from the overnight growth was transferred to 150 ml Tryptone Soya Broth (TSB) medium and was incubated at 37°C with vigorous shaking (150 r.p.m) for 18 h; cell growth was checked by measuring optical density (OD) of the culture at absorbance 600 nm and purity checked by Gram stain.

Disc diffusion

Antibacterial activity of *Cerastes cerastes* venom was evaluated according to (10). The surfaces of plates were covered with the bacterial growth for the three bacterial strains which re-suspended and adjusted turbidity to 0.5 McFarland (11). Sterile blank paper discs (5mm diameter) were then placed on plates and 20µl of venom with the concentration of LD_{50} were added per disc in three replicates. Antibiotic discs including Erythromycin (15 µg Oxoid lot no. 1876568) and Ampicillin (10 µg Oxoid lot no. 1843425) were used as positive controls. The plates were incubated at 37°C for 18 hr. and the inhibition zones were measured.

MIC

Minimum inhibitory concentration (MIC) of *Cerastes cerastes* venom was determined according to (12). The venom was prepared in three serial dilutions (1/2 – 1/64) of three plates including LD_{50} (0.535 mg venom/kg body weight), 40 mg venom /1ml saline and 10 mg venom /1ml saline respectively.

Twenty microliters of reconstituted venom were added to 100µl of standard McFarland bacterial growth in a 96 well plate. The bacterial control was made by adding 100 µl inoculated bacterial culture in one well, while negative control was prepared by adding 20 µl of saline to 100µl of standard McFarland bacterial growth. In order to compare the antibacterial effect of the venom with a standard antibiotic, 100µl of antibiotic was pipette as a positive control. The microplates were incubated at 37°C for 24h. Then plates were read on ELISA reader (Biotek- ELX800-USA) at wavelength 600 nm.

Experimental animals:

Forty-five apparently adult Swiss albino mice, 5 – 7 weeks old, weighing 20±5 were

used. Mice were obtained from the Animal House Facility of the Egyptian Organization for Biological Products and Vaccines, Helwan, Egypt. Mice were housed in standard condition and fed with normal diet and water ad libitum. They were kept in standard conditions of illumination with a 12 h light–dark cycle at 25°C. They were acclimatized to the environment for one week prior to experimental use. The experiments were approved by the state authorities and followed the Egyptian rules on animal protection.

Study design:

Mice were divided into 3 groups as follow:

- Group I: 15 animals were injected subcutaneously with 500µl physiological saline (0.9% NaCl) and served as a control.
- Group II (1/10 LD_{50}):15 mice were injected subcutaneously with 500 µl saline solution containing 1.07µg venom/mouse.
- Group III (1/2 LD_{50}): 15 mice were injected subcutaneously with 500 µl saline solution containing 5.35µg venom/mouse.

Blood collection and analysis

Animals of all groups were sacrificed 48 h post injection and two blood samples were collected. The first sample was collected in EDTA containing tube for RBC, Hb, Hct, platelets and total leukocytes neutrophils and lymphocytes counts analyzed by automated blood counter (colter model T 450 x, Contronics Co., USA). The second blood sample allowed to stand for 30min then centrifuged at 3000 rpm for 10 min. Serum was collected and stored at –20°C. The following biochemical parameters were measured in the control and treated groups: Determination of transaminases (ALT and AST) activities were based on the methods of (13). Creatinine was determined by the method described (14), while urea determined by diacetyl monoxime method as described by (15). Creatine kinase (CK) was determined according to the method of Gella *et al*., (1985) (13). Finally, lactate dehydrogenase (LDH) was determined following (16).

Histopathological studies:

After dissecting the mice, liver, heart, skin, and kidney tissues were removed and fixed in neutral buffered formalin 10%, washed in tap water overnight and exposed to ascending concentrations of ethanol (70, 80, 90 and 100%), cleared in Xylene and embedded in paraffin. Sections of the tissues (4-5 µ thick) were prepared and stained with Hematoxylin and Eosin (H&E) for subsequent histopathological examinations (17). They were examined under a complex Olympus light microscope and photographed by a built-in camera.

Statistical analysis

The analysis was done using SPSS (version 16, Chicago, IL, USA); all results were expressed as the mean ± S.D. The data were analyzed by one-way analysis of variance (ANOVA). To compare the difference between the groups, post hoc testing is performed by the least significant difference (LSD). The $P \geq 0.05$ is considered statistically significant (18).

3. Results:

3.1. Determination of half lethal dose (LD_{50}):

Figure (1) showed the approximate half lethal dose (LD_{50}) of *Cerastes cerastes* venom that assessed according to (9).

LD_{50} = 10.7 µg/mouse (0.535 mg/kg body weight)

3.2. In vitro Antibacterial activity

To assess the antibacterial activity of *Cerastes cerastes* venom, we used the disc diffusion method with LD_{50} of venom and also two different standard antibiotics against three different strains of bacteria. From this initial screening, *E. coli* bacteria were found to be resistant to LD_{50} of the venom as no inhibition zone was exhibited in the antibacterial assay. However, standard antibiotics were shown to be effective (Table 1).

In contrast, the venom was effective against *Staphylococcus aureus* and *Salmonella typhimurium*: maximum inhibitory zones were 13.5 and 13mm on average, respectively, in four experimental repeats. While the averages of inhibition zone of Ampicillin on both of these two bacteria were 21 and 25 mm respectively, for Erythromycin the average of inhibition zones were 8mm (Table 1).

The minimum inhibitory concentration (MIC) determined on the susceptible bacteria, *Staphylococcus aureus* and *Salmonella*

typhimurium, was 62.5 µg/ ml and 125 µg/ ml of venom respectively for both strains. The assays were performed in three replicates.

Two sublethal doses of *C. cerastes* venom (1/10 LD_{50} and 1/2 LD_{50}) were injected into two groups of mice in order to evaluate their toxicological effect, and decide the applicability of such venom as an antibacterial agent for different pathogenic and multidrug-resistant strains.

3.3. In vivo Hematological results:

In the present study, mice envenomed with *C. cerastes* crude venom at 1/10 LD_{50} and 1/2 LD_{50} doses caused different changes of the selected Hematological parameters. The results in the table (2) showed a highly significant increase ($p \leq 0.001$) in Hb, WBCs, RBCs, and platelet counts in both 1/10 LD_{50} and 1/2 LD_{50} groups as compared to control group**.** Hct showed a non-significant increase in 1/10 LD_{50} as compared to control. While when comparing 1/2 LD_{50} group with 1/10 LD_{50} there were highly significant decrease ($p \leq 0.001$) in Hb, Hct, RBCs and platelet counts, and highly significant increase in WBCs count.

Results revealed a highly significant increase ($p \leq 0.001$) in monocyte and eosinophil of 1/10 LD_{50} as compared to control group, while neutrophils and lymphocytes were decreased significantly in the same group. Meanwhile, 1/2 LD_{50} group showed a highly significant ($p \leq 0.001$) increase in the above-mentioned parameters in comparison with both the control and 1/10 LD_{50} groups (Table 3).

3.4. Biochemical results:

Table (4) showed a highly significant increase ($p \leq 0.001$) in the levels of ALT, AST, CPK, LDH, creatinine, and blood urea nitrogen as compared to control**.** Also, 1/2 LD_{50} samples exhibited a highly significant elevation in all parameters as compared to 1/10 LD_{50} group.

3.5. Histopathological results:

Control skin (fig. 2A) consisting of epidermal layer, the dermal layer consisting of connective tissue that contains many hair follicles and fat cells of hypodermis, the underneath muscle fibers is noted. The skin of mice from 1/10 LD_{50} group showed separation of the uppermost layer of the epidermis and early signs of dermal edema and collagen fibers degeneration (fig. 2B). While skin from 1/2 LD_{50} group showed degeneration of hair follicle, degeneration of collagen fibers and advanced edema that separate epidermal and dermal layers, sloughing of the uppermost layer of the epidermis, degeneration of muscle fibers and focal necrosis of dermis (fig. 2C&D).

Mice liver from control group revealed the normal histological structure of normal hepatocytes, centrally located nucleus arranged around central vein and blood sinusoid with kupffer cell (fig. 3A). Meanwhile, liver sections of mice from 1/10 LD_{50} group showed dilated central vein with many mono-nuclear lymphocyte infiltrations, swollen hepatocyte with karyolitic and Pyknotic nuclei (fig. 3 B1&B2). However, mice liver from 1/2 LD_{50} group showed dilated sinusoid with kupffer cells, many Pyknotic nuclei and lymphocyte infiltration (fig.3C1). Congested dilated central vein surrounded by massive lymphocyte infiltration and large necrotic area with many Pyknotic nuclei (fig.3C2). Cytoplasmic vacuolization of hepatocytes, focal necrosis, and focal hepatic hemorrhage observed (fig. 3C3).

The examination of kidney cortex from control group showed a normal histological structure of Malpighian corpuscles with its glomerulus and narrow bowman space (fig. 4A). Kidney cortex of mice from 1/10 LD_{50} group showing abnormal, irregular and cleavage of glomerulus with Erythrocytes, also slight width in Bowman's space and slight degeneration in renal tubules was detected (fig. 4B). The 1/2 LD_{50} group showing severe degeneration changes in the cells of cortex tubules, including cytoplasmic vacuolation, several exfoliated nuclei, and loss of brush borders. Shrinking, separation and atrophy of glomeruli form wide Bowman space was observed (fig. 4C)

Mice heart muscle of control group showing normal branched cardiac muscle fiber with centrally located nuclei (fig. 5A)**.** Heart muscles of mice from 1/10 LD_{50} group showing marked severe intramuscular hemorrhage and slightly degenerated myocytes (fig. 5B)**.** Heart of 1/2 LD_{50} group showing focal myonecrosis associated with

inflammatory cells infiltration in between the cardiac myocytes (fig.5C)

4. Discussion

. The bacterial infection especially antibiotic-resistant strains are of the top leading causes of death worldwide (7). Several studies described the antimicrobial effect of snake venoms (19). In the present study, the antibacterial activity of *Cerastes cerastes* crude venom against the selective bacterial strains was evaluated by disc diffusion technique, the venom was effective against Gram-positive bacteria *Staphylococcus aureus* and Gram-negative bacteria *Salmonella typhimurium*. Also, standard antibiotic Ampicillin was a highly effective antibacterial, while Erythromycin showed a moderate antibacterial activity. These results matched with (20) who stated that *C. cerastes* venoms showed broad antibacterial activities against different bacterial strains.

In our results, *C. cerastes* venom showed no antibacterial effects (resistance) against the Gram-negative bacteria *Escherichia coli*. These results are in agreement with (21) who reported that Gram-negative bacteria were more resistant to test crude venoms than Gram-positive bacteria; this may be due to outer membrane charged lipopolysaccharides. Our results also agree with (7). While Shebl *et al*., (2012) (22) reported that *S. aureus* showed the highest susceptibility to the test venoms, followed by *E. coli*. However, *S. typhimurium* exhibited the least susceptibility to venoms. Our study also, showed that the minimum inhibitory concentration (MIC) of venom determined on the susceptible bacteria, *Staphylococcus aureus*, and *Salmonella typhimurium* were 62.5 µg/ ml and 125 µg/ ml respectively. These values were greatly higher than that obtained with the standard antibiotics. These results matched the results obtained by (22) who concluded that the use of crude venoms was better than the purified components.

In the current study, the assessment of LD_{50} of the *Cerastes cerastes* crude venom was recorded 10.7 µg/mouse or (0.535 mg/kg body weight) by the intravenous route using 20 g Swiss mice. These results conducted with that obtained by (23). Snake venoms are good sources of molecules for drug discovery that have potential applications in medicine (24).

In this study, an increase in Hb and RBCs count was reported in 1/10 LD_{50} envenomed group as compared to saline control group. While, a high reduction observed in Hb, RBCs, HCT and platelet in 1/2 LD_{50} envenomed group. These results were consistent with (25). In this study also, there was a significant increase in MCH and MCHC in 1/10 LD_{50} group and a high reduction of which in 1/2 LD_{50} group was recorded. A decrease in RBCs and platelets counts in our study revealed that the clotting by platelets arose to resist hemorrhage and then dropped with RBCs. Also, the decrease in RBCs count observed in 1/2 LD_{50} group might be due to the stress of envenomation as stated by (26).

In our study, a highly significant increase in white blood cell count in mice from both 1/10 and 1/2 LD_{50} groups was observed. Leukocytosis enhanced by *C. cerastes* venom could be due to inflammation and toxicity as a result of venom components (27).

As liver enzymes (ALT and AST) are common markers for cellular damage, the results of this study clearly revealed that a single injection of *C. cerastes* crude venom at a dose of 1/10 and 1/2 LD_{50} caused a highly significant increase in ALT and AST enzymes which was higher in 1/2 LD_{50} group. This increase indicates that liver is the primary target of venom components and a hepatic damage takes place with *Cerastes cerastes* venom. This result agreed with (28) who observed the increases of ALT and AST enzyme activities in rats injected with a single dose of venom (*Cerastes cerastes*) at a dose of 1/4, 1/2 LD_{50} and LD_{50}.

Our data showed a highly significant increase in serum creatinine and urea in mice from both 1/10 and 1/2 LD_{50} groups indicating histological changes in the kidney of treated mice with *C. cerastes* venom. Our results are supported by (29). In our study also, a highly significant increase in the levels of cardiac enzymes CPK and LDH in mice from both 1/10 and 1/2 LD_{50} groups is observed. This result matched with (30).

Histopathological examination of the skin of 1/10 LD_{50} group 48 hours post-injection showed few histopathological lesions which were progressed in the 1/2 LD_{50} group

in the form of sloughing of the uppermost layer of the epidermis, advanced edema separating epidermal and dermal layers and degeneration of some hair follicle, myonecrosis, and fat necrosis (4) reported similar results with the same venom.

In our study, the histoarchitecture of liver sections in 1/10 LD_{50} group showed dilated central vein with lymphocyte infiltration and moderate necrosis. However, examined sections of mice livers from 1/2 LD_{50} group showed severe changes as, congested dilated central vein with lymphocyte infiltration, focal necrosis, and focal hepatic hemorrhage. This change was coordinated with the increase in liver enzymes. This supported by (31). Our results demonstrated that the kidney cortex in 1/10 LD_{50} treated group showed abnormal glomerulus, a slight width in Bowman space and slight degeneration in renal tubules. While in 1/2 LD_{50} group, there are severe degeneration changes in the cells of cortex tubules. These results indicate the high uptake of the venom by the kidney, our results also, matched with (31)

In the present study, the histopathological examination of the mice heart muscles in 1/10 LD_{50} group showed severe intermuscular hemorrhage and slightly degenerated myocytes, while the heart of mice from 1/2 LD_{50} group induced myonecrosis associated with inflammatory cells infiltration between the cardiac myocytes. These results agree with (4,30).

In conclusion, the results indicated that *C. cerastes* crude venom has broad antibacterial activity on *Salmonella typhi* and *Staphylococcus aureus* in vitro. On the other hand, the histopathological changes that occurred in skin, liver, heart and kidney tissues, as well as the biochemical parameters, indicate a slight effect of a single dose of 1/10 LD_{50} of *C. cerastes* venom than 1/2 LD_{50} after 48 hours of injection.

References

1- Al-Sadoon, M. K., Abdel-Moneim, A. E., Bauomy, A. A., & Diab, M. M. (2013a). Histochemical and Biochemical effects induced by LD_{50} of *Cerastes cerastes gasperetti* crude venom in mice. *Life Sci J*, *10*, 810-817.

2- Al-Sadoon, M. K., & Paray, B. A. (2016). Ecological aspects of the horned viper, *Cerastes cerastes gasperetti* in the central region of Saudi Arabia. *Saudi journal of biological sciences*, *23*(1), 135-138.

3- Berling, I., & Isbister, G. K. (2015). Prolonged QT risk assessment in antipsychotic overdose using the QT nomogram. *Annals of emergency medicine*, *66*(2), 154-164.

4- Boumaiza, S., Oussedik-Oumehdi, H., & Laraba-Djebari, F. (2016). Pathophysiological effects of *Cerastes cerastes* and Vipera lebetina venoms: Immunoneutralization using anti-native and anti-60 Co irradiated venoms. *Biologicals*, *44*(1), 1-11.

5- Vyas, V. K., Brahmbhatt, K., Bhatt, H., & Parmar, U. (2013). Therapeutic potential of snake venom in cancer therapy: current perspectives. *Asian Pacific journal of tropical biomedicine*, *3*(2), 156-162.

6- Rajkumar, S., Sistla, S., Manoharan, M., Sugumar, M., Nagasundaram, N., Parija, S. C., ... & Walia, K. (2017). Prevalence and genetic mechanisms of antimicrobial resistance in Staphylococcus species: A multicentre report of the indian council of medical research antimicrobial resistance surveillance network. *Indian Journal of Medical Microbiology*, *35*(1), 53.

7- Al-Asmari, A. K., Abbasmanthiri, R., Osman, N. M. A., Siddiqui, Y., Al-Bannah, F. A., Al-Rawi, A. M., & Al-Asmari, S. A. (2015). Assessment of the Antimicrobial Activity of Few Saudi Arabian Snake Venoms. *The open microbiology journal*, *9*, 18.

8- Hanane-Fadila, Z. M., & Fatima, L. D. (2014). Purification, Characterization and Antibacterial Activity of l-amino Acid Oxidase from *Cerastes cerastes*. *Journal of biochemical and molecular toxicology*, *28*(8), 347-354.

9- Reed, L. J., & Muench, H. (1938). A simple method of estimating fifty percent end points 1 2. American journal of epidemiology, 27(3), 493-497.

10- Bauer, A. W., Kirby, W. M., Sherris, J. C., & Turck, M. (1966). Antibiotic

susceptibility testing by a standardized single disk method. *American journal of clinical pathology*, *45*(4), 493.

11- McFarland, J. (1907). The nephelometer: an instrument for estimating the number of bacteria in suspensions used for calculating the opsonic index and for vaccines. *Journal of the American Medical Association*, *49*(14), 1176-1178.

12- Andrews, J. M. (2001). Determination of minimum inhibitory concentrations. *Journal of antimicrobial Chemotherapy*, *48*(suppl 1), 5-16.

13- Gella, F. J., Olivella, T., Pastor, M. C., Arenas, J., Moreno, R., Durban, R., & Gomez, J. A. (1985). A simple procedure for the routine determination of aspartate aminotransferase and alanine aminotransferase with pyridoxal phosphate. *Clinica chimica acta*, *153*(3), 241-247.

14- Bartels, H., Böhmer, M., & Heierli, C. (1972). Serum creatinine determination without protein precipitation. *Clinica chimica acta; international journal of clinical chemistry*, *37*, 193-197.

15- Natelson, S. (1971). Total cholesterol procedure (libermann burchard reagent) or free fattyacids in serum. *Techniques of clinical chemistry*, 263-268.

16- Tietz, N. W. (1976). Fundamentals of Clinical Chemistry, Saunders, Philadelphia. *Sec. Edit*, *876*.

17- Bancroft, G. D., Stevens, A., & Turner, D. R. (1996). Theory and practice of histological techniques. *Churchill: Livingston. New York*.

18- Härdle, W., & Simar, L. (2007). Principal components analysis. *Applied Multivariate Statistical Analysis*, 215-249.

19- Samy, R. P., Stiles, B. G., Chinnathambi, A., Zayed, M. E., Alharbi, S. A., Franco, O. L., ... & Sethi, G. (2015). Viperatoxin-II: A novel viper venom protein as an effective bactericidal agent. *FEBS open bio*, *5*(1), 928-941.

20- Hafshejani, F. B., & Jamshidi, A. (2009). Investigation of the antibacterial effect of venom of the Iranian snake *Cerastes cerastes*. In *Third Iranian Congress of Clinical Microbiology*.

21- San, T. M., Vejayan, J., Shanmugan, K., & Ibrahim, H. (2010). Screening antimicrobial activity of venoms from snakes commonly found in malaysia. *Journal of applied sciences*, *10*(19), 2328-2332.

22- Shebl, R. I., Mohamed, A. F., Ali, A. E., & Amin, M. A. (2012). Antimicrobial Profile of Selected Snake Venoms and Their Associated Enzymatic Activities. *British Microbiology Research Journal*, *2(4), 251-263.*

23- Oukkache, N., Jaoudi, R. E., Ghalim, N., Chgoury, F., Bouhaouala, B., Mdaghri, N. E., & Sabatier, J. M. (2014). Evaluation of the lethal potency of scorpion and snake venoms and comparison between intraperitoneal and intravenous injection routes. *Toxins*, *6*(6), 1873-1881.

24- Suntravat, M., Nuchprayoon, I., & Pérez, J. C. (2010). Comparative study of anticoagulant and procoagulant properties of 28 snake venoms from families Elapidae, Viperidae, and purified Russell's viper venom-factor X activator (RVV-X). *Toxicon*, *56*(4), 544-553.

25- Al-Sadoon, M. K., & Haffor, A. S. A. (2005). The effect of *Cerastes cerastes gasperetti* venom on hepatocyte mitochondria ultrastructure and blood cell count. *Journal of Medical Sciences*, *5*(4), 253-259.

26- Riaz, Z., Zaman, M. Q., Ullah, H. U. R., Yousaf, M. S., Rabbani, I., Khan, I., ... & Majeed, K. A. (2015). Bio-physiological effects of LD_{50} of crude venom of black pakistaní cobra (*Naja Naja karachiensis*) in mice. *JAPS, Journal of Animal and Plant Sciences*, *25*(5), 1344-1348.

27- Al-Sadoon, M. K., & Fahim, A. (2012). Possible recovery from an acute envenomation in male rats with LD_{50} of Echis coloratus crude venom: IA seven days hematological follow-up study. *Saudi journal of biological sciences*, *19*(2), 221-227.

28- Bashandy, M. A., Abd-El-Aal, A., Ibrahim, D. F., & El-Sharkawy, M. A. (2016).

29- Protective effects of date palm extract as natural antioxidants on hepatotoxicity induced by *Cerastes cerastes* venom in albino rats. *International Journal of Advanced Research*, *4*(3), 647-665.
30- Saleh, S. M., & Kasem, N. R. (2016). Toxicological Effects of Viper Cerastes cerastes Crude Venom on Serum Indices of Male Albino Rats. *Journal of Forensic*, *1*(2), 13.
31- Oukkache, N., Lalaoui, M., & Ghalim, N. (2012). General characterization of venom from the Moroccan snakes Macrovipera mauritanica and Cerastes cerastes. *Journal of Venomous Animals and Toxins including Tropical Diseases*, *18*(4), 411-420.
32- Al-Sadoon, M. K., Abdel Moneim, A. E., Diab, M. M., & Bauomy, A. A. (2013b). Hepatic and renal tissue damages induced by *Cerastes cerastes gasperetti* crude venom. *Life Sci. J*, *10*(4), 191-197.

Table 1: *In vitro* antibacterial activity of *Cerastes cerastes* crude venom against selected bacterial strains using disc diffusion method and compared to two antibiotics. Mean bacterial inhibition zone diameter (mm) ± SD.

Micro-organism / Venom / Antibiotics	***S. aureus***	***E. coli***	***S. typhi***
***C. cerastes* venom (0.535µg/g)**	13.5mm ± 0.11	0.0 ± 0.0	13mm ± 0.02
***Ampicillin* (10 µg/ml)**	21mm ± 0.09	22mm ± 0.12	25mm ± 0.07
***Erythromycin (*15 µg/ml)**	8mm ± 0.00	10mm ± 0.03	8mm ± 0.05

Table (2): Blood parameters of Hematology of mice in different studied groups (n: number of mice).

Parameters / Groups and doses		Hb (g/dl)	RBCs ($\times 10^6$/ µl)	HCT (%)	MCV (fl)	MCH (Pg)	MCHC (g/dl)	Platelets ($\times 10^3$ / µl)	WBCs ($\times 10^3$ / µl)
Control (n= 15)	Mean± SE	11.47 ±0.084	7.8 ± 0.133	40.02±0.737	51.44 ±1.19	14.59 ± 0.24	28.60±0.593	374.4 ± 10.50	6.21 ± 0.055
	SD	0.328	0.516	2.85	4.63	0.931	2.29	40.69	0.216
1/10 LD_{50} (1.07 µg /mouse) (n= 15)	Mean± SE	13.18 ±0.104	8.45 ±0.105	41.34 ± 0.50	48.95 ±0.80	15.57±0.197	31.88±0.399	58.93 ± 3.14	7.5 ± 0.258
	SD	0.408	0.406	1.93	3.09	0.76	1.54	12.16	0.999
	P value	0.000	0.000	0.128	0.049	0.005	0.000	0.000	0.000
	% change a	(↑ 14.9%)	(↑ 8.3%)	(↑ 3.3%)	(↓ 4.8%)	(↑ 6.5%)	(↑11.4%)	(↓ 84.3%)	(↑20.8%)
1/2 LD_{50} (5.35 µg /mouse) (n= 15)	Mean± SE	9.5 ± 0.136	6.2 ± 0.098	36.0±0.525	31.63±0.43	11.5±0.247	25.0±0.487	43.86 ± 0.42	11.42 ±0.244
	SD	0.529	0.379	2.03	1.69	0.958	1.88	1.64	0.945
	P value	0.000	0.000	0.000	0.000	0.000	0.000	0.000	0.000
	*P** value	0.000	0.000	0.000	0.000	0.000	0.000	0.100	0.000
	% change a	(↓17.2%)	(↓ 20.5%)	(↓10.0%)	(↓ 38.5%)	(↓ 21.3%)	(↓ 10.7%)	(↓88.28%)	(↑ 83.89%)

Table 3: Differential Blood cells of mice in different studied groups (n: number of mice).

Parameters / Groups and doses		Lymph (%)	Segmented Neutrophils (%)	Staff cell Neutrophils (%)	Mono (%)	Eosinophil (%)	Basophil (%)
Control (n= 15)	Mean± SE	55.4 ± 0.518	39.2±0.72	1 ± 0.125	3.0 ± 0.25	1.33±0.125	0.00±0.00
	SD	2.0	2.8	0.48	1.0	0.48	0.00
1/10 LD_{50} (1.07 µg /mouse) (n= 15)	Mean± SE	52 ± 0.64	37.33 ± 0.73	2.06 ± 0.24	6.0±0.21	4.8 ± 0.26	0.00±0.00
	SD	2.5	2.84	0.96	0.84	1.0	0.00
	P value	0.002	0.005	0.029	0.000	0.000	1.00
	% change a	(↓ 6.13%)	(↓ 4.77%)	(↑ 106%)	(↑ 100%)	(↑ 260.9%)	0.00%
1/2 LD_{50} (5.35 µg /mouse) (n= 15)	Mean± SE	68 ± 0.61	45.0±0.52	3.06±0.28	9.86±0.37	9.86 ± 0.45	1.4 ± 0.28
	SD	2.39	2.0	1.0	1.45	1.76	1.12
	P value	0.000	0.000	0.000	0.000	0.000	0.000
	*P** value	0.000	0.000	0.004	0.000	0.000	0.000
	% change a	(↑ 22.74%)	(↑ 14.79%)	(↑206%)	(↑228. 6%)	(↑641.35%)	(↑ 140%)

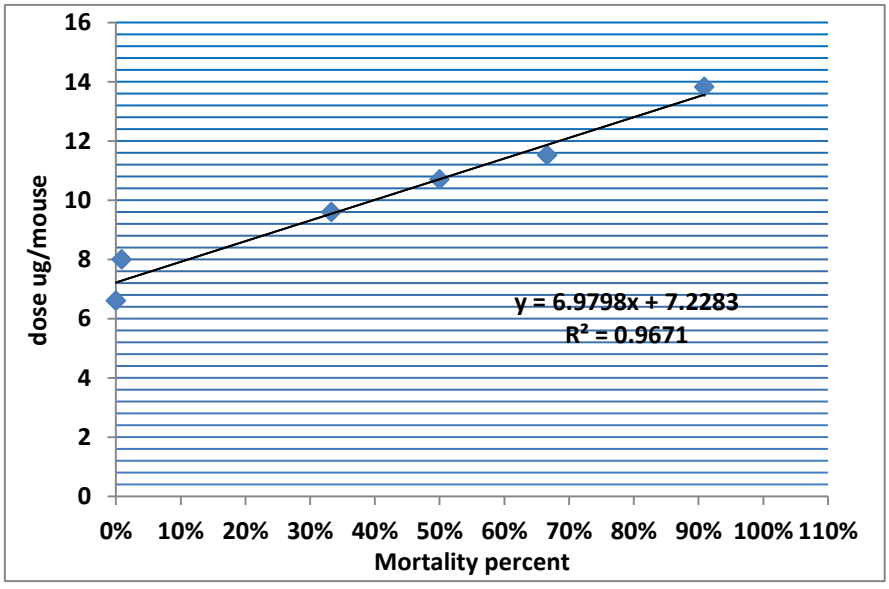

Figure 1. Mortality curve of Swiss Albino mice administrated different doses of *C. cerastes* venom.

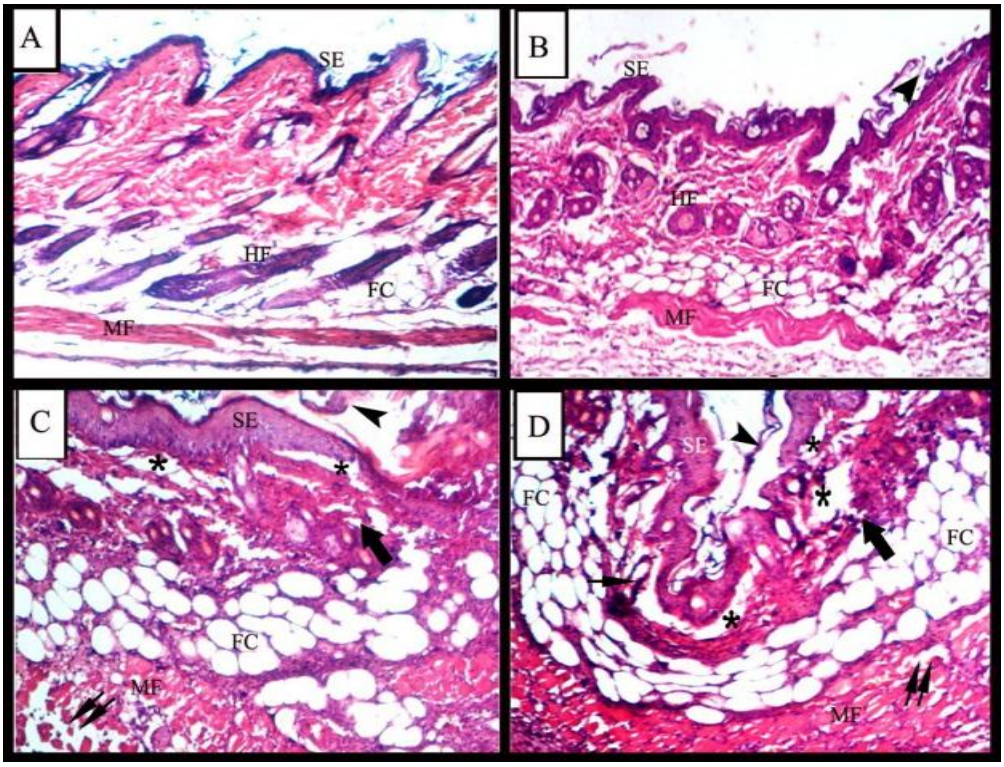

Figure 2. Photomicrograph of mice skin

A) Photomicrograph of mice skin from control group showing normal histological structure consisting of epidermal layer (stratified squamous epithelium SE), dermal layer consisting of connective tissue that containing many hair follicles (HF) and fat cells (FC) of hypodermis, note the underneath muscle fibers (MF) (H&E X 200). **B)** The skin of mice from 1/10 LD_{50} group showing separation of the uppermost layer of epidermis (arrow head) and early signs of dermal edema and collagen fibers degeneration (arrow). (H&E X 200). **C & D)** explained histological changes of skin from 1/2 LD_{50} group, where there was degeneration of hair follicle (arrow), degeneration of collagen fibers and advanced edema that separate epidermal and dermal layers (*), sloughing of the uppermost layer of epidermis (arrow head), degeneration of muscle fibers (double arrow) and focal necrosis of dermis (thick arrow). (H&E X200).

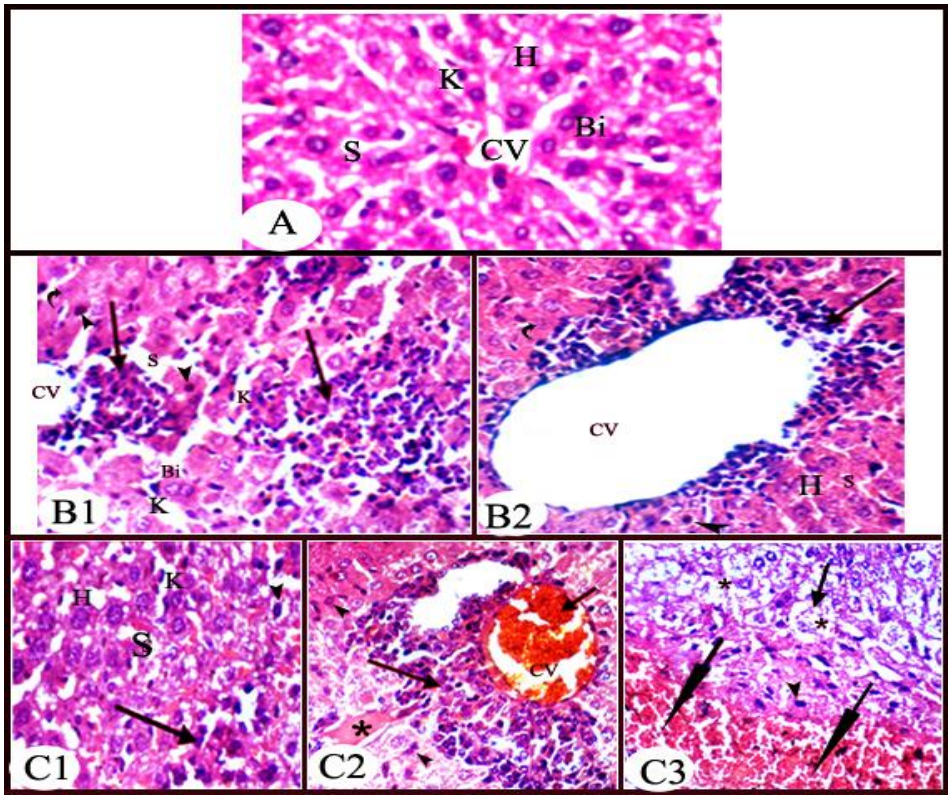

Figure 3. Photomicrograph of the liver

A) Photomicrograph of the liver of control group showing normal histological structure of normal hepatocytes (H), central located nucleus arranged around central vein (CV) and blood sinusoid (S) with kupffer cell (K). Note: bi-nucleated cell (Bi). (H&E X200). **B1, B2)** Showing liver sections of 1/10 LD_{50} group, **B1)** showing large necrotic area with focal lymphocyte infiltration and dilated blood sinusoid (S) with many kupffer cells (K). **(B1 & B2):** showing dilated central vein (CV) with mono-nuclear lymphocyte infiltration (arrow), swollen hepatocyte with karyolitic (bent arrow) and Pyknotic (arrow head) nuclei (H&E X200). **C1, C2, C3)** Examined sections of mice livers from 1/2 LD_{50} group, **C1)** showing dilated sinusoid (S) with kupffer cells (K), many Pyknotic nuclei (arrow head) and lymphocyte infiltration (arrow). **C2)** showing congested dilated central vein (CV) surrounded by massive lymphocyte infiltration (arrow) and large necrotic area (*) with many Pyknotic nuclei (arrow head). Also **C3)** showed cytoplasmic vacuolization of hepatocytes (short arrow), focal necrosis (*) and focal hepatic haemorrhage (long arrow). (H&E X200).

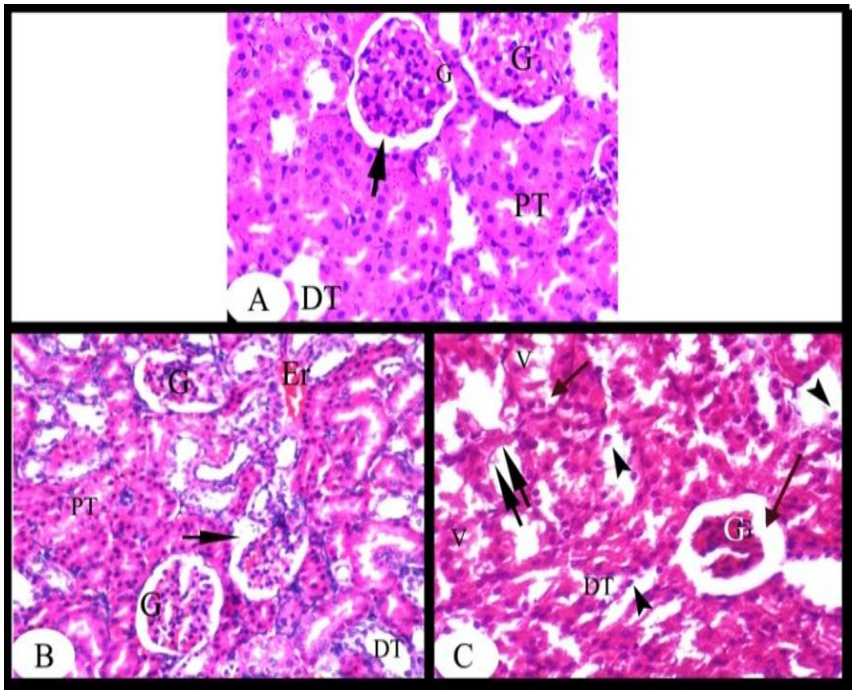

Figure 4. Photomicrograph of cross section in Kidney cortex

A) Photomicrograph of cross section in Kidney cortex of control group in mice showing normal histological structure of Malpighian corpuscles with its glomerulus (G) surround by narrow Bowman space (arrow). Note: proximal tubules (PT) and distal tubule (DT), (H & E X 200). **B)** Photomicrograph of Kidney cortex of mice from *Cerastes cerastes* group II (1/10 LD_{50}) showing abnormal irregular and cleavage glomerulus with Erythrocytes (ER), and slightly wider bowman space (arrow). Note: Slightly degenerated renal tubules (PT& DT), (H & E X 200). **C)** Photomicrogaph of Kidney cortex of mice from *Cerastes cerastes* group III (1/2 LD_{50}) showing severe degeneration changes in the cells of cortex tubules, include: cytoplasmic vaculation (V), several exfoliated nuclei (arrow head), and loss of brush borders (double arrow). Shrinking, separation and atrophy of glomerulei (G) form wider Bowman space (arrow). (H&E X200).

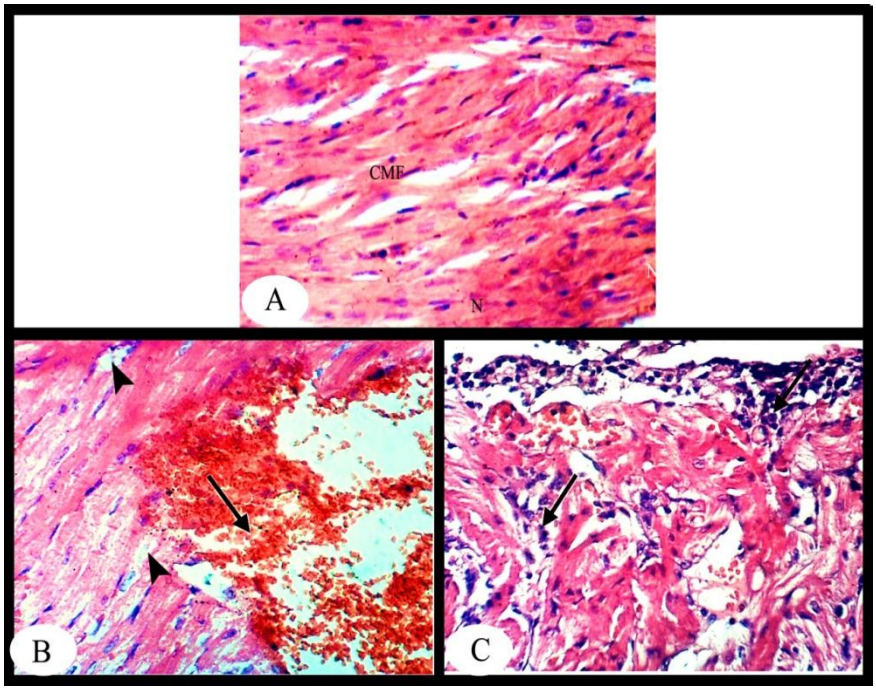

Figure 5. Photomicrograph of mice heart muscle

A) Photomicrograph of mice heart muscle of Control group showing normal branched cardiac muscle fiber with centrally located nuclei (CMF) (H & E X 200). **B)** Heart muscles of mice from 1/10 LD_{50} of *Cerastes cerastes* treated group showing marked severe intermuscular haemorrhage (arrow) and slightly degenerated myocytes (arrowhead) (H & E X 200). **C)** Heart of mice from 1/2 LD_{50} of *Cerastes cerastes* treated group showing focal necrosis of cardiac myocytes (myonecrosis) associated with inflammatory cells infiltration in between the cardiac myocytes, (arrow),(H & E X200).